Building and Environment 291 (2026) 114235

Contents lists available at ScienceDirect

Building and Environment

journal homepage: www.elsevier.com/locate/buildenv

Precooling effectiveness in residential buildings during heatwaves with power outages: A sensitivity and parametric analysis

Xue Liu [a], Hao Tang [b], Xuyuan Kang [c], Pengyuan Shen [d], Xin Zhou [e], Da Yan [c,*]

[a] School of Architecture, Southwest Jiaotong University, Chengdu 611756, China
[b] Institute of Smart City and Intelligent Transportation, Southwest Jiaotong University, Chengdu 611756, China
[c] Building Energy Research Center, School of Architecture, Tsinghua University, Beijing 100084, China
[d] Institute of Future Human Habitats, Shenzhen International Graduate School, Tsinghua University, Shenzhen, Guangdong Province, China
[e] School of Architecture, Southeast University, Nanjing, Jiangsu Province 210096, China

ARTICLE INFO

Keywords:
Precooling
Heatwave
Outage
Thermal resilience
Optimization
Sensitivity analysis

ABSTRACT

Climate change is increasing the frequency and intensity of heatwaves, often accompanied by power outages that exacerbate indoor overheating and threaten human health. Precooling is a potential mitigation strategy for indoor overheating risks; however, few studies have systematically explored the impact of building design, cooling capacity, and power-outage events on its performance. This study proposes an optimized precooling thermostat schedule using Bayesian optimization to minimize thermal discomfort and cooling electricity costs. Based on this strategy, Sobol sensitivity and parametric analyses were conducted to explore the effects and interactions of building design parameters, cooling capacity, and power outage characteristics on thermal discomfort and electricity costs. A prototype high-rise residential building in Chengdu, China, was used as a case study. The results showed that thermal discomfort during power outages was primarily influenced by external wall insulation, airtightness and internal thermal mass, whereas cooling electricity cost was mainly affected by airtightness. Furthermore, the contribution of the internal thermal mass to reducing thermal discomfort increased with cooling capacity, whereas the influence of airtightness diminished. This suggests that coordinated optimization between cooling capacity and internal thermal mass is more effective than merely oversizing the cooling system. Regarding power outage impacts, the optimized precooling strategy maintained acceptable indoor comfort for approximately 6 h during morning outages, while only 2 h during afternoon outages. These findings offer practical guidance for policymakers and residents seeking to maximize the benefits of precooling strategies during heatwaves with power outages.

1. Introduction

Global climate change has significantly increased the frequency, intensity, and duration of heatwaves in several parts of the world [1]. This global trend is manifested as extreme heatwaves in various regions. For instance, in the UK, the daily maximum temperature exceeded 40 °C for the first time on record in 2022 [2]. In China, the average number of high-temperature days per year (daily maximum temperature $\geq$ 35 °C) has steadily increased over the past decades, from a historical average of nine days to 16 days in 2022 [3]. The increasing frequency and severity of heatwaves have sharply increased building cooling demand, posing serious challenges to power supply reliability. Heatwaves can increase the likelihood of power outages and prolong their duration [4]. A notable example is the 2022 Heatwave in Sichuan, China. According to the Lancet Countdown 2023 report, the prolonged heatwave in 2022 in the Sichuan region is expected to lead to a surge in cooling demand, whereas drought conditions will reduce hydropower generation, resulting in electricity rationing in the region [5].

Heatwaves accompanied by power outages can lead to a substantial increase in indoor temperatures, significantly increasing the risk of overheating in buildings. This issue is particularly critical in residential buildings and vulnerable facilities, as populations such as the elderly, children, and individuals with preexisting health conditions, who typically spend more time at home, are especially susceptible to heat-related risks [6,7]. Previous studies have shown that when mechanical cooling is disrupted during heatwave events, indoor heat index levels can

* Corresponding author.
E-mail address: yanda@tsinghua.edu.cn (D. Yan).

https://doi.org/10.1016/j.buildenv.2026.114235
Received 5 September 2025; Received in revised form 1 January 2026; Accepted 10 January 2026
Available online 11 January 2026

escalate into the "danger" or even "extreme danger" zones, substantially raising the likelihood of heat exhaustion, heat stroke, and other heat-related illnesses [8–10]. Consequently, it is essential for governments, utility companies, and residents to take proactive measures to enhance thermal resilience and mitigate the overheating risks posed by heatwaves combined with power outages [11].

Precooling has been recognized as a potential solution for improving thermal resilience during heatwave events with power outages. This technique has been applied in demand response programs to shift cooling loads from peak to off-peak hours by utilizing the thermal mass of a building to store cooling energy in advance and release it later. Typically, this is implemented by lowering the thermostat setpoint a few hours before peak periods and increasing it during peak hours [12]. By slowing the rate of increase in the indoor air temperature, precooling makes it possible to reduce or avoid air conditioning (AC) operation during on-peak periods. Notably, this strategy requires no additional equipment or significant modifications to the existing AC systems, making it relatively easy to implement in existing buildings. Moreover, precooling may provide economic benefits because it enables residents to take advantage of time-of-use electricity pricing by shifting part of the cooling load to lower-cost periods [13].

Numerous studies have demonstrated that precooling can effectively shift cooling loads from peak to off-peak hours, enhance peak load reduction, reduce energy costs, and maintain indoor thermal comfort [13]. These studies mostly used residential [14–18] and office buildings [19–22] as case studies. Turner et al. assessed the precooling performance of a one-story house with a light thermal mass across various U.S. climate zones [14]. Their results showed that all the tested precooling strategies successfully shifted at least 50 % of the peak-period cooling loads to off-peak hours. Similarly, Stopps and Touchie simulated precooling and preheating setback controls for load shifting in high-rise residential buildings in Canada and found that control strategy performance varied among suites owing to differences in occupant behavior [15]. They further recommended limiting the maximum temperature setback during load shifting control to 3 °C to prevent frequent occupant overrides [16]. Wang et al. developed an optimized precooling strategy for a test house to minimize energy costs, achieving up to 50 % cost savings compared with rule-based methods [23]. In addition to simulation-based analyses, a few studies have employed field tests or experimental methods to validate the effectiveness of precooling. Yin et al. conducted field tests in 11 commercial buildings and observed peak-period electricity demand reductions of 15–30 % [24]. Chen et al. examined the potential of passive thermal mass and active storage systems in demand response programs using precooling and found that passive thermal mass was effective for short-term events (up to 2 h), whereas active storage was necessary for longer events [25]. Jiang et al. conducted a four-month long-term field test in nine houses to evaluate a model-predicted control-based precooling strategy, and the results showed that the energy cost could be reduced by 28.7–51.3 % on hot summer days [18]. These simulations and field studies demonstrate the potential of precooling to reduce the peak loads and energy costs in demand response programs. However, the aforementioned studies were primarily conducted in the context of demand response, aiming to reduce electricity consumption or minimize electricity costs, with indoor thermal comfort being used as a constraint. These studies were conducted under scenarios with uninterrupted power supply and continuous air-conditioning operation.

In addition to evaluating the effectiveness of precooling measures, several studies have investigated the potential factors influencing their performance, including building insulation, structural and internal thermal mass, AC system capacity, time-of-use electricity pricing, and climate conditions. For example, Wang et al. investigated the influence of the cooling capacity on precooling strategies across three capacity levels and found that increasing the cooling capacity shortened the AC system runtime but had little effect on the cooling energy consumption or cost [17]. Lu et al. conducted a parametric analysis to analyze the effects of thermal mass, weather conditions, and energy prices on the precooling performance [20]. Their results showed that buildings with a heavy thermal mass offered greater potential for cost savings and peak load reduction, albeit with an associated energy penalty. Their study focused primarily on flexible cooling load management in commercial buildings. Reza et al. analyzed the impact of various energy efficiency measures on the energy cost of a precooling strategy and found that roof insulation and lighting power density had the largest impact on energy costs [26].

In summary, existing studies have extensively examined the effectiveness of precooling in reducing peak loads and lowering energy costs and have developed optimized operating schedules to achieve these objectives. However, limited research has addressed the precooling performance under combined heatwave and power-outage scenarios. For example, one study evaluated the precooling effectiveness during heatwaves, but the AC system remained in continuous operation, which did not reflect the constraints under power-outage conditions [27]. Another study focusing on California suggested that heatwave-related power outages longer than 2 h substantially increased the risk of indoor overheating; however, this conclusion was based on conventional AC operation without implementing precooling measures [28]. Therefore, these two research questions remained unaddressed. The first is the feasibility of applying precooling during heatwaves with power outages and the extent to which precooling performance is influenced by various factors in residential buildings. To address these questions, this study developed an optimized precooling thermostat scheduling method using a Bayesian optimization algorithm, aiming to minimize both indoor overheating risks during outages and the economic burden on residents. Second, sensitivity and parametric analysis was conducted to quantify the impacts of the building design parameters, cooling capacity, and outage event characteristics on overheating and energy cost. These findings guide both policymakers and residents to maximize the benefits of precooling strategies for reducing indoor overheating risks during such events.

2. Methodology

The methodology of this study consisted of three primary steps, as illustrated in Fig. 1. The first is the setting of the scenario. The scenario set in this study was a historical five-day heatwave and power-outage event. A prototype high-rise residential building was selected as a case study. This scenario provides the simulation boundary conditions and outage profiles used as inputs for the subsequent strategy development. The second step was to develop an optimized precooling strategy and evaluate its performance related to thermal discomfort and energy costs. Finally, the impacts of building design parameters, cooling capacity, and characteristics of power-outage events on the efficacy of precooling were investigated using global sensitivity and parametric analyses.

2.1. Scenario setting

2.1.1. Weather data

The selection of heatwave events follows the definition proposed by the China Meteorological Administration, where a heatwave was defined as a period of three consecutive days with the daily maximum temperatures exceeding 35 °C [29]. Chengdu experienced a severe heatwave from August 8 to 24, 2022. A continuous five-day period was selected from this event, during which the daily maximum temperature exceeded 38 °C. The dry-bulb temperature and relative humidity of the selected heatwaves are shown in Fig. 2. Weather data for the selected heatwaves were collected from the ERA5 dataset. ERA5 is a fifth-generation reanalysis climate database produced by the European Center for Medium-Range Weather Forecasts model, which has been widely used for building simulation analysis [30]. The original meteorological variables provided by the ERA5 dataset included the dry-bulb temperature, dew point temperature, 10 m wind over the Earth's

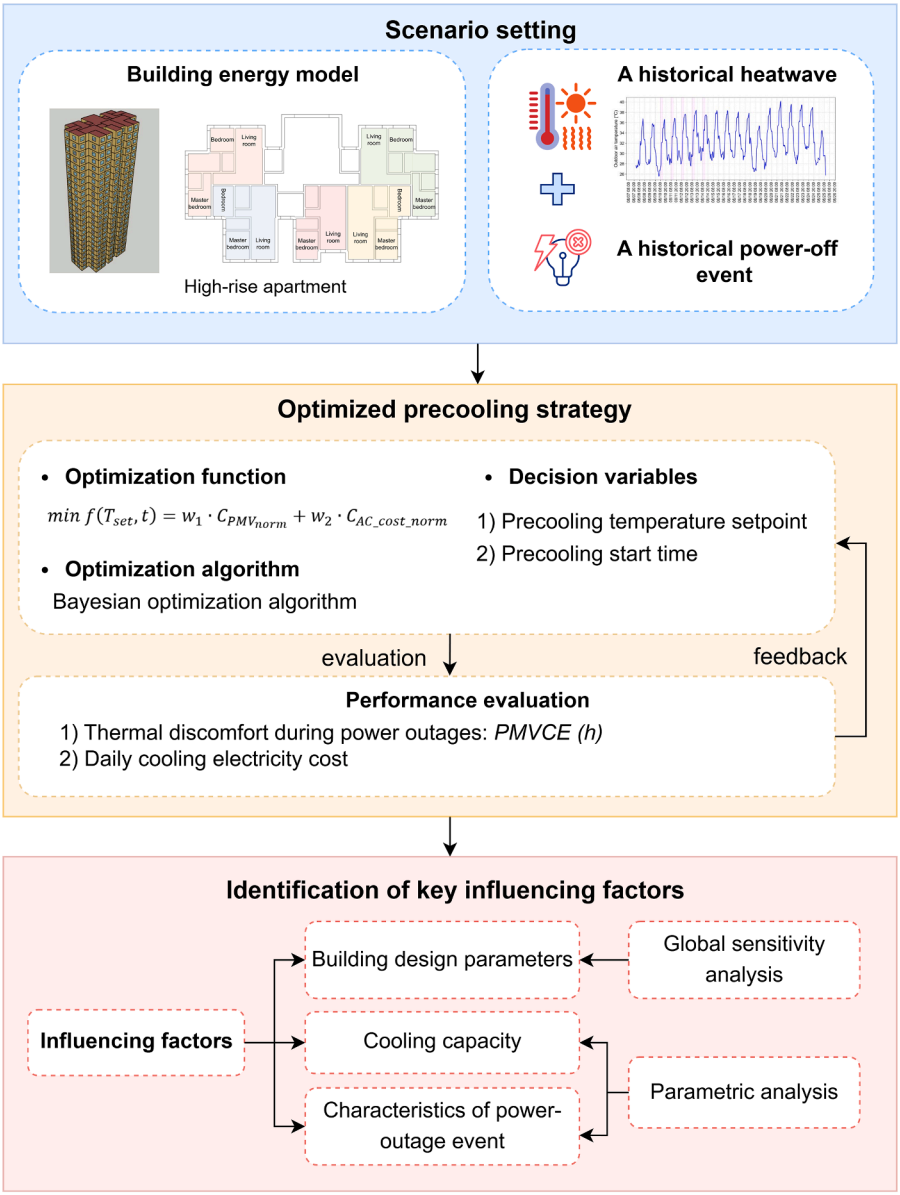

Fig. 1. Methodology framework for this study.

surface, global horizontal irradiance, and direct normal irradiance.

2.1.2. Building energy model

This study selected a prototype high-rise tower residential building in a hot summer and cold winter climate zone (Chengdu, China) to evaluate the optimized precooling framework and conduct a sensitivity analysis. High-rise apartments are one of the most typical housing types, particularly in megacities with large populations. The geometric model and layout of the prototype building are shown in Fig. 3. Each apartment consisted of several types of zones, including residential bedrooms, living rooms, kitchens, and bathrooms.

The building envelope thermal properties of the prototype buildings were set according to the building energy efficiency standard for hot summer and cold winter climate zones released in 2010, as listed in Table 1. The airtightness was set to 0.6 ACH, assuming that the room remains air-conditioned for most of the time except during power outages, and occupants are unlikely to open windows under such conditions to minimize heat exchange with the outdoor environment. This value also fell within the typical range of air change rates established in a previous study on representative residential building models [31]. In terms of the internal heat gain, a typical household was assumed to contain two adults. Occupancy schedules are determined based on a typical daily routine in which at least one person is assumed to remain at home throughout the day [32]. The lighting and electric equipment schedules follow the occupancy patterns. In addition, this study also analyzed the impact of a 10 % increase in internal heat gains on the precooling performance. The detailed results of this analysis are presented in Appendix A.

For the AC system, this case study applied a split air conditioner, which is a typical AC system in residential buildings. In each household, the living room and bedroom were equipped with split air conditioners. The living room had an area of 24 m^2, and the default cooling capacity was set to 3.6 kW. Once the cooling capacity was determined, precooling strategies were implemented based on this capacity. Furthermore, the default setting of internal thermal mass of furniture is 98,010 J/(m^2·K), and the surface area was twice the floor area. These values are adopted from previous studies [27,33].

This study used EnergyPlus v24.2, a simulation engine, to develop the building energy model. This simulation tool, supported by the United States Department of Energy, and is an open-source program that

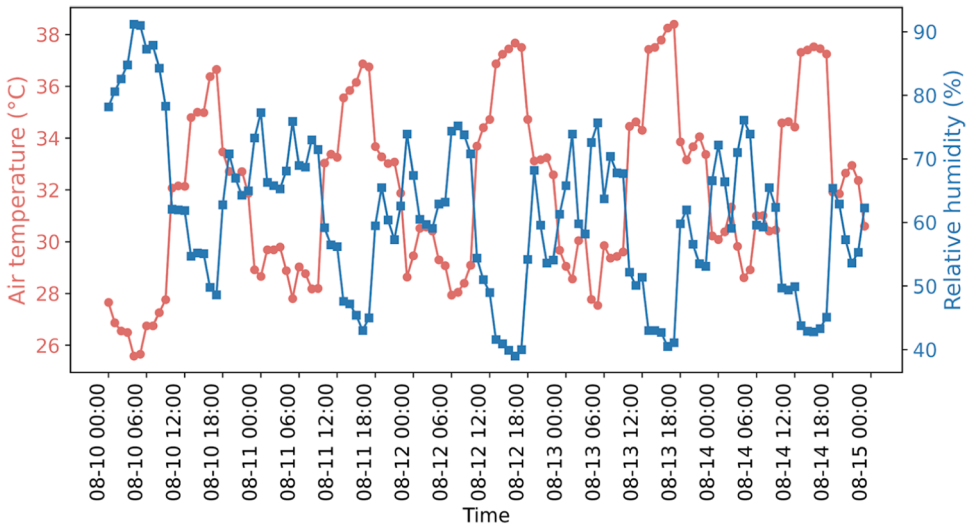

Fig. 2. Outdoor air temperature and relative humidity of the selected heatwave.

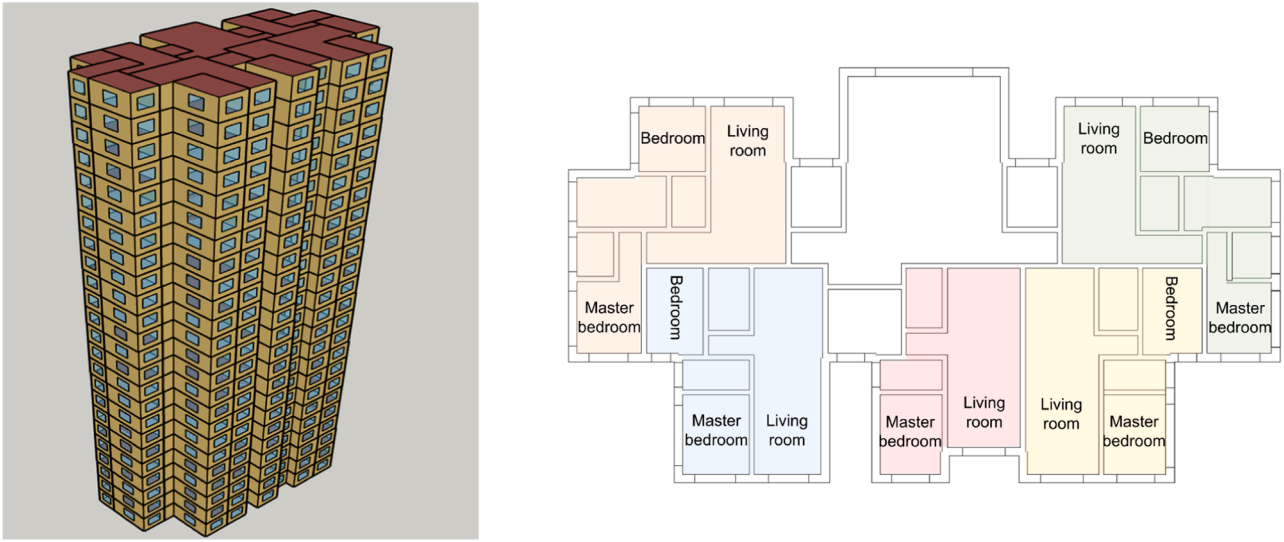

Fig. 3. Geometric model and floorplan of the prototype building.

Table 1
Key parameters for building energy modeling.

Parameters	Value
Average window-to-wall ratio [−]	0.27
U-value of exterior wall [W/(m^2·K)]	0.8
U-value exterior window [W/(m^2·K)]	3.0
U-value of roof [W/(m^2·K)]	1.0
Window SHGC	0.3
Lighting power density [W/m^2]	4.0
Equipment power density [W/m^2]	5.0
Airtightness [ACH]	0.6
Rated cooling capacity [kW]	3.6
Air conditioner COP [−]	3.0
Default cooling setpoint [°C]	25

models heating, ventilation, cooling, lighting, water use, renewable energy generation, and other building energy flows.

2.2. Optimized precooling strategy

An optimized precooling strategy was developed for a historical five-day heatwave event that coincided with a power outage in 2022. The power-outage event lasted from 7:00 to 13:00. The precooling strategy was implemented using a day-ahead rolling optimization scheme in which the optimal temperature setpoints and start time were generated each day based on the daily weather conditions and internal heat gain profiles. It should be noted that precooling was applied only to the living room because nighttime precooling could affect the thermal comfort of occupants' sleep in the bedroom. Besides, occupants are likely to naturally choose the room that offers the most comfortable thermal environment, which would most probably be the pre-cooled living room. Therefore, occupants were assumed to most probably stay in the living room during periods of power outages.

2.2.1. Optimization problem formulation

To optimize the precooling strategy of a residential thermal zone during summer mornings, a multi-objective optimization problem was formulated to minimize the daily cooling electricity cost and thermal discomfort. The decision variables included the precooling temperature setpoint and start time. Once precooling begins, the air conditioner operates continuously until a power outage begins, maintaining a constant thermostat setpoint to maximize thermal storage. The objective

function is defined as shown in Eq. (1). This formulation seeks to determine the globally optimal precooling setpoint and start time within the optimization horizon.

$$min\, f(T_{set}, t) = w_1 \cdot C_{PMV_{norm}} + w_2 \cdot C_{AC\_cost\_norm} \quad (1)$$

Here, T_{set} denotes the precooling temperature setpoint (°C) during the precooling period and serves as a decision variable. It is constrained between 20.0 °C and 26.0 °C, with a resolution of 0.5 °C. The variable t represents the start time of pre-cooling, ranging from 01:00–07:00, with a resolution of 0.5 h. C_{PMV_norm} is the normalized thermal discomfort measured by the predicted mean vote (PMV), as shown in Equation (2); $C_{AC\_cost\_norm}$ is the normalized daily electricity cost (CNY) of the AC system and accounts for the dynamic electricity pricing and cooling energy consumed, as shown in Eq. (3). The two objective terms in the optimization function, including thermal discomfort and daily cooling electricity cost, were normalized before aggregation to eliminate the influence of unit differences and ensure comparability. The weighting factors w_1 and w_2 refer to the relative significance of minimizing energy cost and maintaining thermal comfort, respectively. In this study, both weights were set to one ($w_1 = w_2 = 0.5$) to give equal significance to energy cost and thermal comfort in the optimization process. In addition, the effects of different combinations of weighting coefficients on the precooling optimization outcomes were examined. A sensitivity analysis was conducted by varying the relative weighting between the two objectives, and the comparison result is provided in Appendix B.

$$C_{PMV_{norm}} = \frac{PMVCE - PMVCE_{min}}{PMVCE_{max} - PMVCE_{min}} \quad (2)$$

$$C_{AC\_cost\_norm} = \frac{E_{AC} - E_{AC\_min}}{E_{AC\_max} - E_{AC\_min}} \quad (3)$$

$$PMVCE = \int_{t_1}^{t_2} max(0, PMV(t) - PMV_{th})dt \quad (4)$$

Here, *PMVCE* is the cumulative predicted mean vote exceedance hour, defined as a metric for quantifying indoor thermal discomfort. t_1 and t_2 denote the start and end times of the power outage (h), respectively, and PMV_{th} denotes the *PMV* threshold for thermal comfort. In this study, PMV was calculated assuming a metabolic rate of 1.2 met, clothing insulation of 0.5 clo, and air velocity of 0.15 m/s, while the mean radiant temperature was taken from the EnergyPlus simulation results. PMV_{th} was set to 0.7, based on the comfort zone defined by ISO 7730 [34]. $PMVCE_{max}$ and $PMVCE_{min}$ denote the maximum and minimum values of *PMVCE*, respectively; E_{AC} represents the daily total electricity cost; E_{AC_max} and E_{AC_min} indicate the maximum and minimum values of E_{AC}, respectively.

The cooling electricity cost was calculated using the real-time-of-use tariff in Chengdu during the summer of 2022. An off-peak rate of 0.239 CNY/kWh was applied from 23:00 to 07:00; a mid-peak rate of 0.497 CNY/kWh was applied from 07:00 to 14:00 and 21:00 to 23:00; and an on-peak rate of 0.754 CNY/kWh was applied from 14:00 to 21:00.

2.2.2. Optimization algorithm

This study adopts a Bayesian optimization algorithm to solve the optimization problem. The primary motivation for selecting this algorithm was the complexity and computational expense of the building energy model constructed using EnergyPlus. Despite simplifying the optimization problem to only two decision variables, each evaluation still requires an entire building performance simulation, which is time-consuming. Bayesian optimization is a probabilistic global optimization framework that is particularly suitable for problems in which objective evaluations rely on expensive simulations, such as building energy simulations. It uses a probabilistic agent model to approximate the true objective function based on the data obtained from previous evaluations [35]. Bayesian optimization is a type of prior-informed search that leverages the performance of previously evaluated hyperparameters to guide the selection of subsequent candidates. In each iteration, a Gaussian Process was fitted to the observed samples, and the resulting posterior distribution was combined with an acquisition function to determine the next sampling point. This algorithm improves the efficiency of the optimization process by efficiently exploiting historical information. This study used the Bayesian optimization Python package *Bayesian-optimization*. The Bayesian optimization process was initialized with 20 random samples to construct the surrogate model, followed by 50 iterations of guided sampling based on the acquisition function.

2.2.3. Cooling strategies for comparison

To evaluate the performance of the optimized precooling strategy, two additional cooling strategies were selected for comparison. The first is the baseline strategy, in which no precooling is applied. According to the occupied schedule in the living room, the occupied hours are from 09:00 to 21:00, and the desired indoor air temperature in the summer is 25 °C. Therefore, the AC operates from 13:00 to 21:00, as it remains off during the scheduled power outage from 07:00 to 13:00. The temperature setpoint is 25 °C. The second is a fixed precooling strategy, in which the AC is scheduled with a constant setpoint of 25 °C and runs continuously throughout the day, except during the outage period. Table 2 presents a brief introduction to the three cooling strategies.

2.3. Sensitivity and parametric analysis

To investigate the critical factors influencing the effectiveness of precooling during power outage periods, three categories of factors were considered: (1) building design parameters, (2) cooling capacity, and (3) the characteristics of power outage events. Building design parameters involve multiple uncertain variables with potentially nonlinear effects and interactions and were therefore examined using a global sensitivity analysis. The cooling capacity and power-outage events were analyzed using a parametric approach because these factors are characterized by a limited range of representative values.

2.3.1. Sensitivity analysis

Sensitivity analysis can be categorized into two types: local and global. Local sensitivity analysis evaluates the effect of small perturbations in a single input parameter on the output while keeping all other parameters fixed, capturing only the local linear response and failing to reflect nonlinearities or interactions over the full input space [36]. To overcome these limitations, this study employed a global sensitivity analysis using the Sobol method. This variance-based method decomposes the variance of the model output into contributions attributable to individual input parameters and their interactions [37]. The Sobol method defines two critical indices: first-order and total-order. The first-order index is the proportion of the output variance explained by a single parameter, while holding all others fixed. A higher first-order index indicates that the parameter has a strong independent effect on output. However, in high-dimensional problems, first-order indices alone may not fully explain the output variance because the interactions between the parameters can be significant [38]. To address this issue, Saltelli et al. introduced a total-order index that captures the overall contribution of a parameter, including both its direct effect and all interaction effects with other parameters [38]. By comparing the

Table 2
Cooling strategies in this study.

Strategy	AC operation hours	Temperature setpoint (°C)
Baseline	Regular cooling: 13:00–21:00	25
Fixed	00:00–7:00, 13:00–00:00	25
Optimized	Precooling: determined by optimization. Regular cooling: 13:00–21:00	Precooling period: determined by optimization. Regular cooling: 25

first- and total-order indices, it is possible to distinguish between parameters with dominant direct effects and those whose significance arises primarily through interaction effects.

The objective of the sensitivity analysis is to identify the building design parameters that most significantly influence the effectiveness of the precooling strategies. The parameters considered included external envelope insulation, internal thermal mass, and airtightness. Table 3 summarizes the selected parameters and their corresponding ranges, which were determined based on standard building practices and relevant literature. In this study, variations in internal thermal mass were achieved by modifying its surface area, while other properties, such as density and specific heat, remained unchanged. The internal thermal mass ranged from 0.5 to 4 times the room floor area. This range was chosen to represent buildings with varying levels of internal thermal storage, from sparsely furnished to heavily furnished spaces [33]. For the range of airtightness, the air change rate was varied from 0.5 to 3.0 ACH. The lower limit corresponds to the minimum requirement in Chinese standard for indoor air quality in residential buildings, and the upper limit is determined by large-scale airtightness measurements of Chinese residential buildings, which reported that the 95th-percentile air change rate was below 1.5ACH, while the maximum value reached 3.1ACH in summer conditions [39]. Therefore, this study selected 3.0ACH as the upper limit representing older and poor airtightness performance.

Sampling was performed using the Saltelli method, an enhanced sampling strategy typically used in Sobol sensitivity analysis [40]. The samples were generated based on the parameter ranges listed in Table 3. For the Sobol index, the minimum sample size is $N \times (2k + 2)$, where N is the base sample size, ranging from 16, 32, …, 1024, and k is the number of input parameters [40]. In this study, 3072 samples were used, with N set to 256, balancing accuracy and computational cost. Sensitivity analysis was performed using the SALib Python package [41].

2.3.2. Parametric analysis

The cooling capacity of an AC system is a critical factor influencing the effectiveness of precooling strategies. Previous studies have shown that the precooling performance decreases as the AC cooling capacity decreases [27]. To investigate the impact of cooling capacity on precooling effectiveness, five representative cooling capacity levels were considered: 0.5, 0.75, 1.0, 1.25, and 1.5 times the default capacity. These values correspond to 1.8, 2.7, 3.6, 4.5, and 5.4 kW, respectively. Each configuration was analyzed and compared to evaluate its influence on precooling performance in terms of thermal discomfort and electricity cost.

For power outage events, two significant characteristics were considered: the power outage duration and occurrence time. Outage duration refers to the total period during which electricity is unavailable, whereas the time of occurrence indicates the specific time of day when the outage occurs. Both characteristics can directly affect the ability of precooling to maintain thermal comfort during outage periods. Based on these characteristics, three representative outage scenarios are defined as follows:

a) Event 1: Power outage from 07:00 to 13:00 (default case).
b) Event 2: A power outage occurs from 13:00 to 19:00, coinciding with the period of the highest outdoor air temperatures and peak solar radiation. This scenario was intended to evaluate the precooling performance under the most severe weather conditions of the day.
c) Event 3: The outage extended to 12 h, from 07:00 to 19:00. This prolonged blackout scenario was designed to evaluate the effectiveness of precooling strategies under extended outage conditions.

Table 3
Summary of building design parameters.

Parameter	Range
U-value of exterior wall [W/(m^2·K)]	0.3–1.4
U-value of exterior window [W/(m^2·K)]	2.0–6.0
Window SHGC [−]	0.3–0.7
Ratio of internal thermal mass surface area to floor area [−]	0.5–4
Airtightness [ACH]	0.5–3.0

3. Results

3.1. Results of the optimized precooling strategy

During the five-day heatwave, the optimized precooling strategy showed variations in both the temperature setpoint and duration of precooling, as shown in Fig. 4. The temperature setpoint was 20.5 °C on August 11, and 21 °C on August 12 and 13, compared to 20 °C on August 10 and 14. The precooling duration also varied with time. On August 10, 13, and 14, the pre-cooling lasted for 7 h, whereas on August 11 and 12, a shorter duration of 4.5 h was adopted. Notably, although the outdoor temperature on August 10 was not the highest among the five-day heatwave period, the optimized strategy adopted the longest precooling duration with a lower setpoint of 20 °C. This is primarily attributed to the absence of on the preceding day, which leads to internal heat accumulation and requires extended precooling for effective cooling and energy storage.

The simulation results for the indoor air temperature profiles of the baseline, fixed, and optimized precooling strategies are shown in Fig. 5 (a). The baseline scenario had the highest indoor air temperatures, with peak values exceeding 30 °C during the power outage period. The fixed strategy reduced the temperature below 29 °C across the power outages. In contrast, the optimized precooling strategy provided the most effective thermal mitigation, with the indoor air temperature remaining around or even below 27 °C throughout the outage periods, lowering the peak temperatures by up to 3.5 °C compared to the baseline and by 1.7 °C relative to the fixed strategy.

Fig. 5(b) shows the hourly cooling load profiles for the three cooling strategies. The optimized precooling strategy required nighttime operation of air conditioners while significantly lowering the starting cooling load after a power outage compared to the other two strategies. Additionally, the cooling loads during the afternoon period (13:00–21:00) were also lower. These reductions indicate that the building successfully stored a considerable amount of cooling energy in the thermal mass during the precooling periods, effectively decreasing the cooling load during the power recovery periods.

To quantitatively compare the performance of the three different strategies, the electricity consumption, electricity cost, and PMVCE during the heatwave are shown in Fig. 6. The optimized strategy exhibited the highest total electricity consumption owing to the extended operation of the air conditioner during nighttime hours for precooling, with an increase of 41 %. However, this did not correspond to a significant increase in electricity costs because the differences among the three strategies were relatively small. This was primarily because the cooling energy storage during off-peak hours helped reduce cost increases, even though the total energy consumption was higher. Therefore, the optimized precooling strategy did not impose an additional economic burden on the building occupants. The optimized precooling eliminated thermal discomfort during power-outage periods, achieving a 100 % reduction in PMVCE compared with the baseline. This indicates its substantial contribution to maintaining indoor thermal comfort under heatwave conditions. The baseline yielded the highest PMVCE value, indicating the highest overheating risk during power outage periods, while the fixed strategy provided moderate improvement in both cost and thermal comfort but remained less effective than the optimized precooling strategy. Overall, these results demonstrate the effectiveness of the optimized precooling strategy in balancing thermal comfort and cost efficiency despite the higher total electricity consumption.

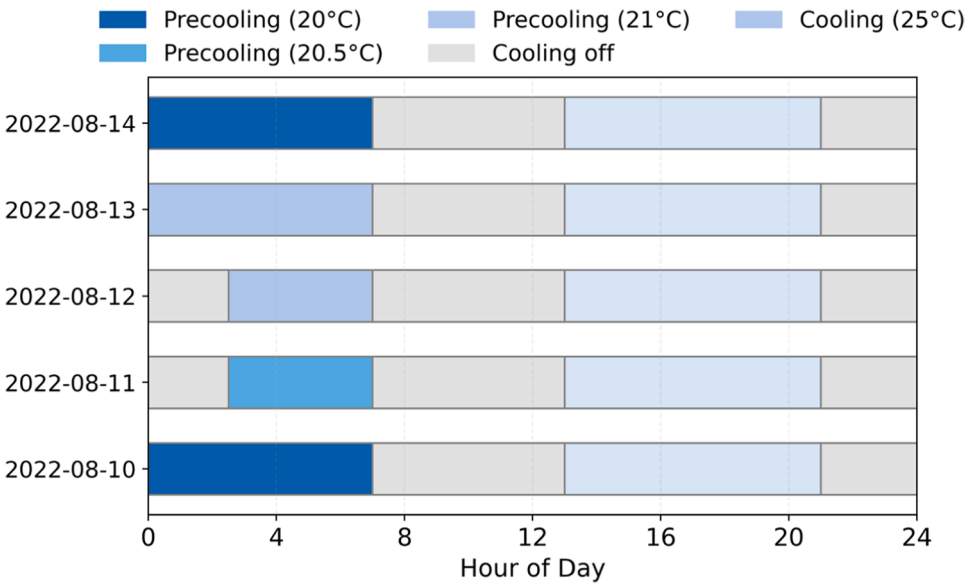

Fig. 4. Cooling schedule of the optimized precooling strategy.

3.2. Impacts of building design parameters

The Sobol sensitivity analysis results for thermal discomfort and electricity costs are presented in Fig. 7. The analyzed input variables included the U-values of the external walls and windows, SHGC, airtightness, and internal thermal mass. These parameters contributed to the variance in thermal discomfort and electricity costs. In this figure, the first-order index represents the direct contribution of each variable to output variance, whereas the total-order index accounts for both the individual effects and their interactions with other variables. A higher Sobol index indicates a stronger influence of input parameters on the output variance. Notably, the differences between the first-order and total-order Sobol indices were small, suggesting that the effects of the parameters were primarily direct rather than that resulting from interactions.

For thermal discomfort, the external wall U-value, internal thermal mass and airtightness were identified as the dominant contributors, with total-order Sobol indices of 0.55, 0.24, 0.22, respectively. The SHGC had a relatively minor effect, with a total-order index of approximately 0.05. In contrast, the electricity cost was predominantly influenced by the airtightness, which had a total-order Sobol index of 0.9, followed by the external wall U-value (0.08), whereas the internal thermal mass and window U-value had negligible effects. These results highlight that external wall insulation, airtightness and internal thermal mass are key to reducing thermal discomfort, whereas airtightness is the dominant factor in cooling electricity costs.

3.3. Impacts of AC cooling capacity

This section investigates the impact of different cooling capacities on the optimized precooling schedule for this building. Fig. 8 illustrates the variation in the precooling setpoints and durations from August 10 to 14 under five different cooling capacity scenarios, corresponding to 1.8, 2.7, 3.6, 4.5, and 5.4 kW. The optimized precooling strategies varied with the cooling capacity. As the cooling capacity increased, the precooling setpoint could be raised or the precooling duration shortened. Nevertheless, once the cooling capacity exceeded 4.5 kW, the optimized precooling strategy remained largely unchanged.

The indoor air temperature and cooling load profiles for the three different cooling capacities are shown in Fig. 9, and the corresponding cooling electricity consumption and costs are summarized in Table 4. The results indicated that cooling capacity primarily affected cooling speed. When the cooling capacity was 1.8 kW, it was sometimes insufficient to reach the desired temperature setpoint during the precooling period. In contrast, cooling capacities of 2.7 kW or higher reduced the indoor air temperature to the setpoint within approximately 2 h, whereas the highest capacity (5.4 kW) reached the setpoint in less than 30 min. This demonstrates that a higher cooling capacity substantially enhances the cooling speed.

However, the effect of the cooling capacity on mitigating indoor overheating and reducing cooling electricity costs was found to be relatively limited. As shown in Fig. 9 and Table 4, except for the 1.8 kW case, the indoor air temperature trajectories during the outage periods were almost identical across different AC sizes, and the PMVCE was reduced to zero. The 1.8 kW case was an exception because the insufficient cooling capacity prevented the setpoint temperature from being consistently reached during nighttime precooling. This resulted in a higher initial air temperature before the outage and, consequently, a greater overheating risk during the subsequent power-outage hours. Regarding electricity consumption and cost, although a higher capacity led to higher instantaneous cooling loads during precooling, the total electricity consumption and associated costs were only slightly affected. Specifically, increasing the cooling capacity from 1.8 kW to 5.4 kW resulted in an approximately 8 % increase in cooling electricity consumption and a 5 % increase in electricity cost.

3.4. Impacts of power-outage events

To further evaluate the effectiveness of the precooling strategy under various power-outage scenarios, two additional events were analyzed. Event 2 represented an afternoon outage (13:00–19:00) with a 6-hour outage duration, during which precooling was conducted from 06:00 to 13:00. At the baseline of this event, air conditioner was assumed to operate from 08:00 to 13:00 and from 19:00 to 21:00, with a temperature setpoint of 25 °C prior to the outage. Event 3 corresponded to a prolonged outage lasting 12 h, from 07:00 to 19:00, with precooling conducted from 0:00 to 07:00. For both events, the optimized precooling strategy was implemented and compared with a no-precooling baseline.

The indoor air temperature and PMV profiles for these two events are shown in Figs. 10 and 11. In Event 2, without precooling, the indoor air temperature exceeded 30 °C, reaching a peak of 30.9 °C. The PMV values rose above +1.0 and even reached +1.5 in some hours. With optimized precooling, the temperature remained basically below 29 °C, with a maximum of 29.5 °C, and the PMV values were generally within +1.0.

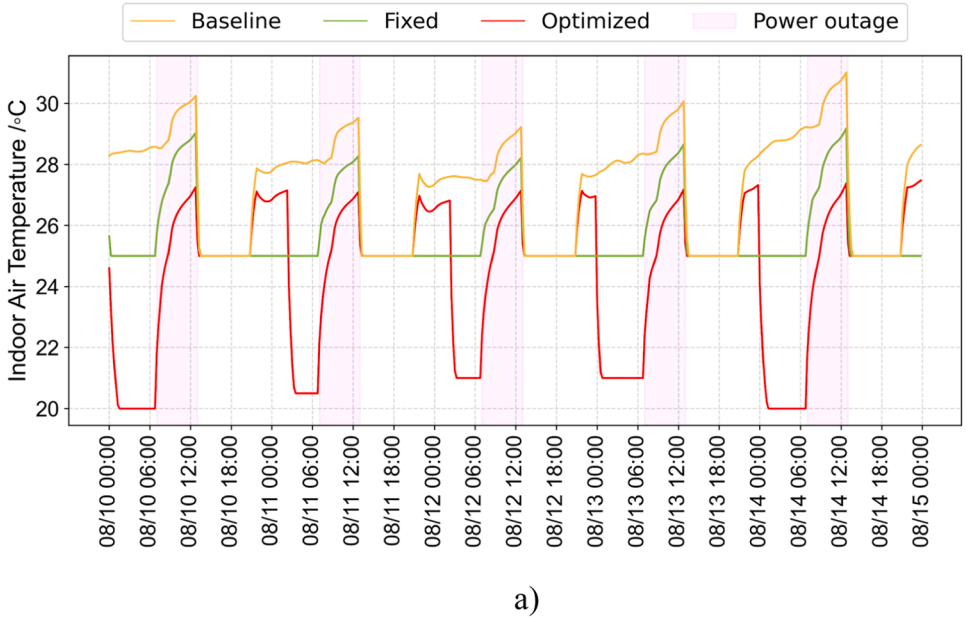

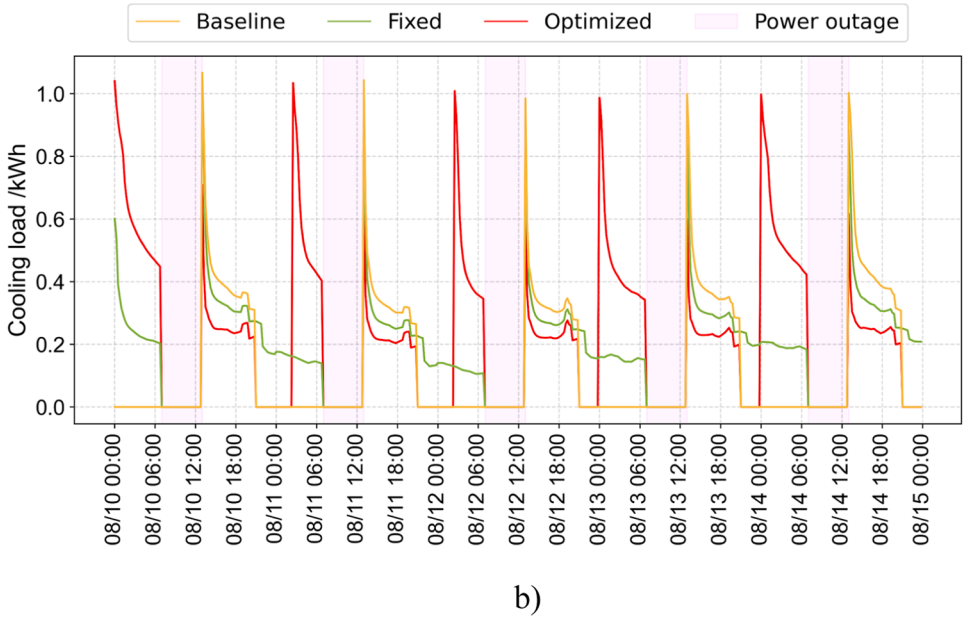

Fig. 5. a) Indoor temperature and b) cooling load profiles of the three cooling strategies.

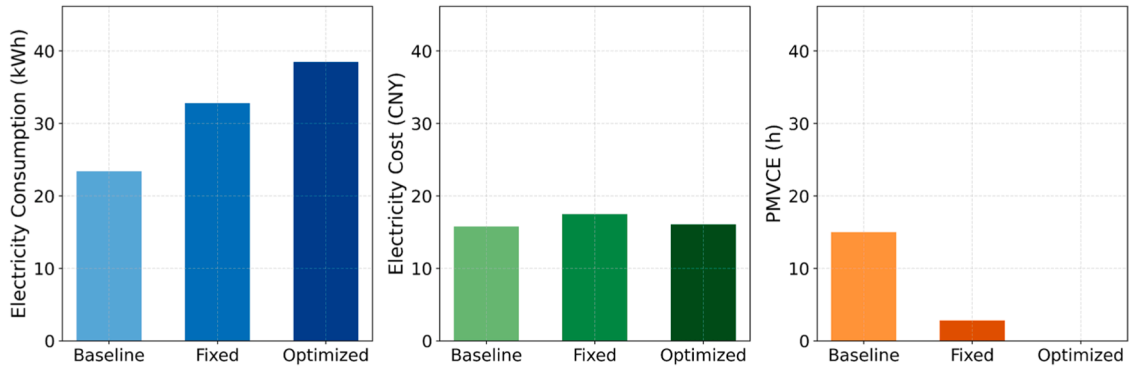

Fig. 6. Electricity consumption, electricity cost, and PMVCE of the three cooling strategies.

Consequently, the PMVCE decreased from 16.4 h to 3.9 h, representing a 76 % reduction, as shown in Fig. 12.

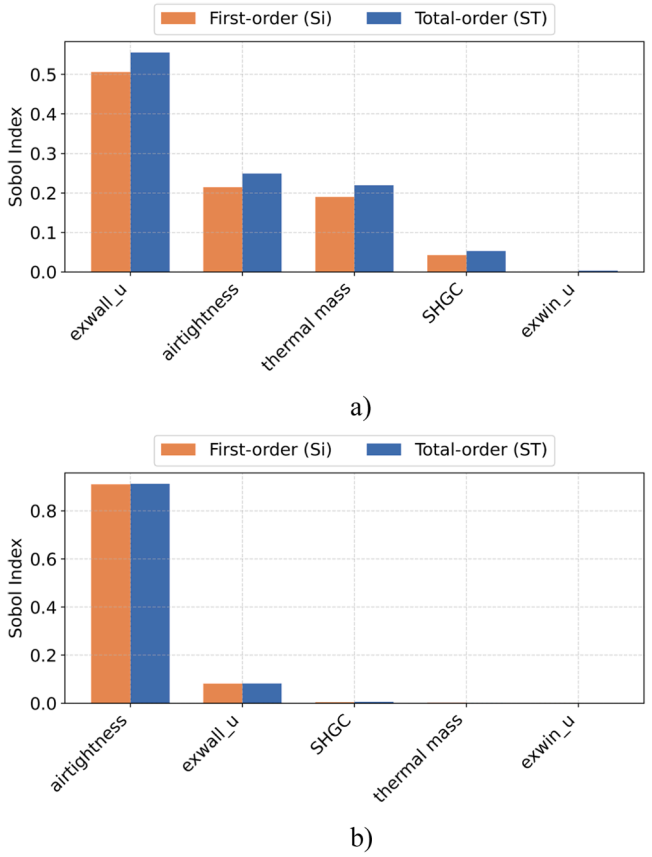

Fig. 7. First- and total-order of the Sobol index of input parameters for a) thermal discomfort and b) energy cost (CNY).

In Event 3, the thermal discomfort became more severe. Without precooling, the PMV exceeded +2.0, indicating a state of heat stress that poses a considerable risk to occupant health. In contrast, with the application of precooling, the indoor thermal risk was significantly mitigated, with PMV peaks maintained around +1.0 and always below +1.5. Accordingly, the PMVCE reduced from 83.9 h to 8.0 h, achieving a 90 % decrease. These results confirmed the effectiveness of optimized precooling in mitigating overheating and enhancing indoor thermal resilience during outages.

The effective duration of thermal comfort maintained by precooling was also analyzed. In Event 2, the acceptable duration of thermal comfort maintenance was approximately 2 h, whereas in Event 1 (07:00–13:00 outage), it was 6 h. This difference reflects the effect of the outage time. For an outage of the same duration beginning in the afternoon, precooling is less effective owing to higher outdoor air temperatures and greater solar gains. In Event 3, when the power outage occurred in the morning and lasted 12 h, precooling could maintain the indoor conditions within the comfort zone for approximately 6 h, except on the first day, when it lasted only approximately 2 h. However, after 13:00, the indoor PMV values increased sharply, resulting in the highest level of thermal discomfort.

In terms of electricity consumption and cost, the precooling scenario consumed more electricity than scenarios without precooling. This also led to an increase in power costs, with a 28 % increase in electricity costs for Event 2 and 46 % increase in electricity costs for Event 3. Among the three events, Event 2 exhibited the highest electricity cost, primarily because precooling was conducted during daytime hours when electricity prices were relatively higher.

4. Discussion

4.1. Explanation of the impacts of building design parameters

The results of the Sobol sensitivity analysis show that the primary factors influencing thermal discomfort and electricity costs related to the precooling performance are distinct. External wall insulation is the dominant contributor to thermal discomfort, followed by internal thermal mass. During power outages, heat transfer through external walls dominates the cooling energy loss, increasing both the indoor air temperature and the mean radiant temperature, thereby exacerbating thermal discomfort. Airtightness can increase thermal discomfort through air exchange; however, its impact is relatively minor in this study because of the upper limit considered (3.0 ACH). Internal thermal mass primarily affects thermal discomfort by storing cooling energy during precooling and slowing the rate of temperature rise as it shifts, rather than reducing cooling demand.

Airtightness was identified as the primary contributor to electricity cost. Poor airtightness accelerates the loss of cooled indoor air and the infiltration of hot outdoor air, thereby increasing the cooling demand and electricity consumption. In addition, it introduces additional latent heat, which further increases the cooling load. The influence of external wall insulation on electricity costs was relatively small. This is primarily because of the thermal inertia of both the walls and the internal thermal mass; when leveraged through precooling, the buffer temperature rises and mitigates the peak cooling demand.

To place the results of this study into a broader research context, the main sensitivity analysis findings are compared with those reported in previous studies focusing on similar precooling applications. For

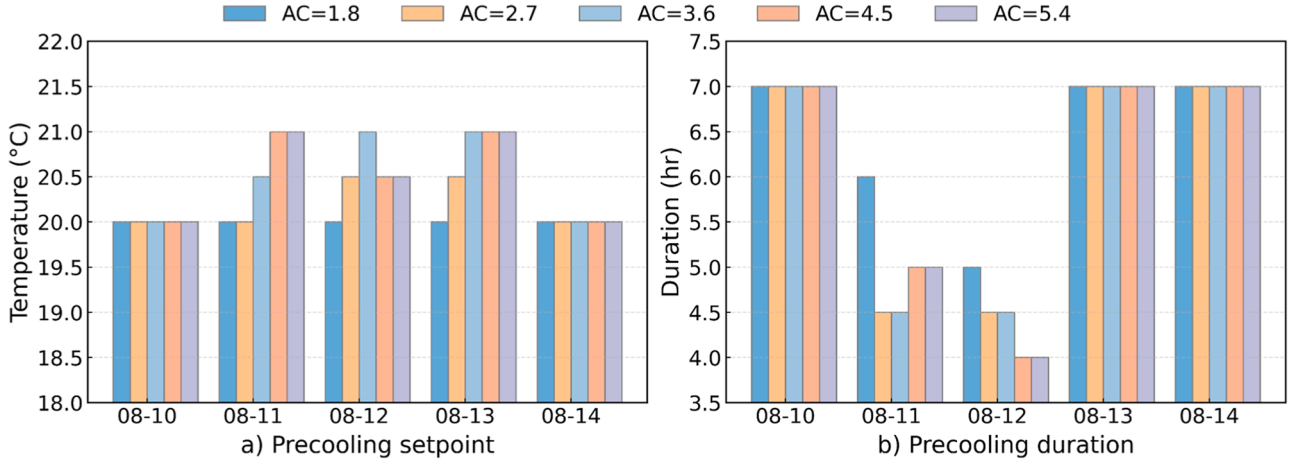

Fig. 8. Optimized precooling strategies under varying cooling capacities.

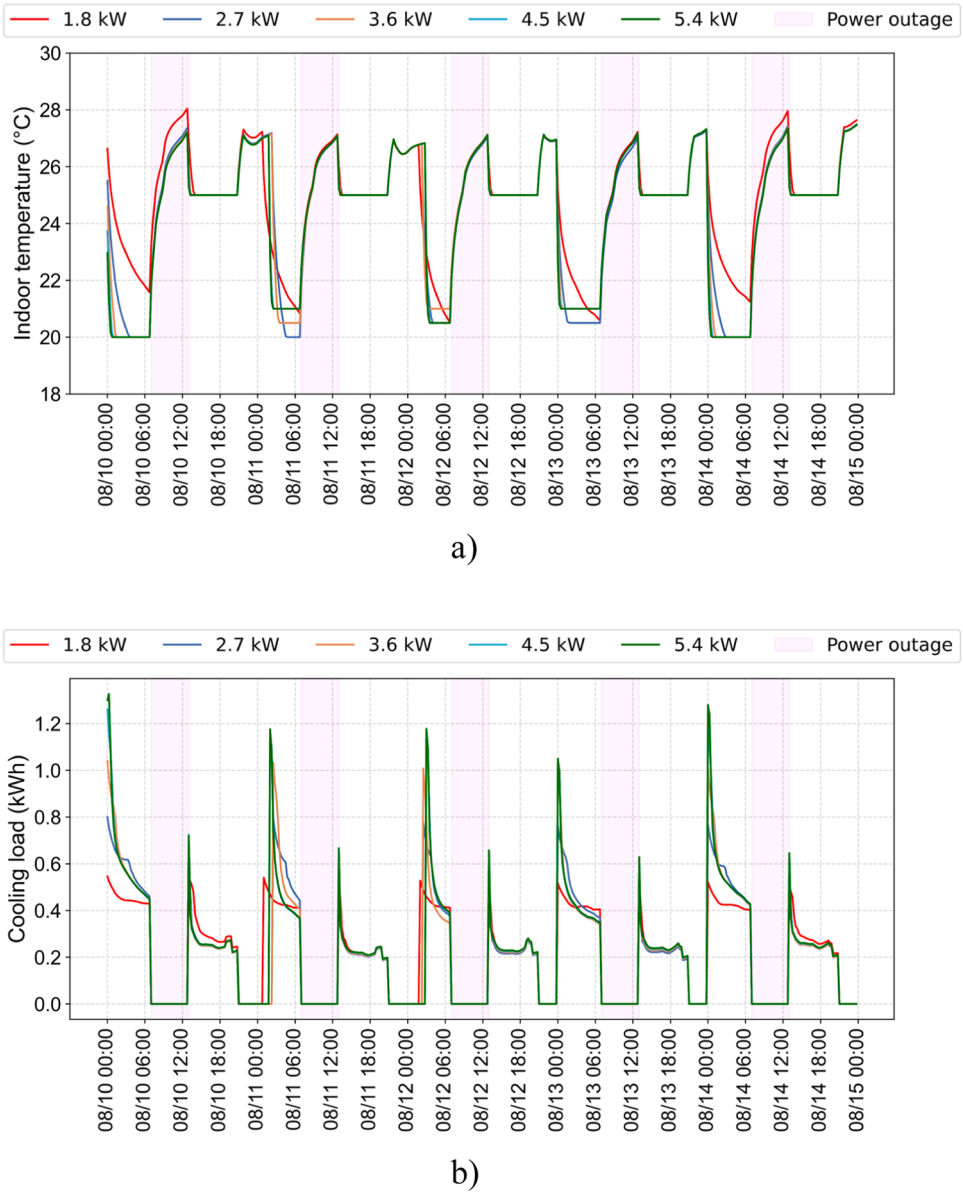

Fig. 9. a) Indoor air temperature and b) cooling load profiles under different cooling capacities.

Table 4
Electricity consumption, electricity cost, and PMVCE of the optimized precooling strategy under three cooling capacities.

Cooling capacity (kW)	Electricity consumption (kWh)	Electricity cost (CNY)	PMVCE
1.8	36.1	15.8	0.32
2.7	38.3	15.9	0
3.6	38.5	16.0	0
4.5	39.1	16.3	0
5.4	39.3	16.4	0

instance, a comparable study conducted in Australia reported that peak-load reduction potential of precooling exhibited a strong sensitivity to star-rating levels, reflecting improvements in both envelope performance and airtightness can benefit precooling performance [42]. However, the study did not identify which specific envelope improvements had the most important effect on peak-load reduction or cost outcomes. Another similar study compared precooling performance related to energy cost savings and peak load reduction under light, medium and heavy thermal mass configurations, and found heavy thermal mass was the most effective [20]. In comparison, the findings in this study also reflect the effects of thermal mass on improving thermal discomfort during power outages.

4.2. Sensitivity analysis under different cooling capacities

Fig. 13 presents the Sobol total-order sensitivity index of the parameters under the five cooling capacities. For thermal discomfort, the external wall insulation consistently played a dominant role, whereas the influence of airtightness decreased and that of the internal thermal mass increased with a higher cooling capacity. At a low cooling capacity (e.g., 1.8 kW), airtightness plays a more significant role than the internal thermal mass because the limited cooling output makes indoor temperatures highly sensitive to infiltration. As the cooling capacity increased (e.g., 3.6 kW), enhanced precooling and greater thermal storage utilization reduced this sensitivity, highlighting the need to coordinate the cooling capacity with passive thermal characteristics to fully leverage the benefits of precooling. Regarding the electricity cost,

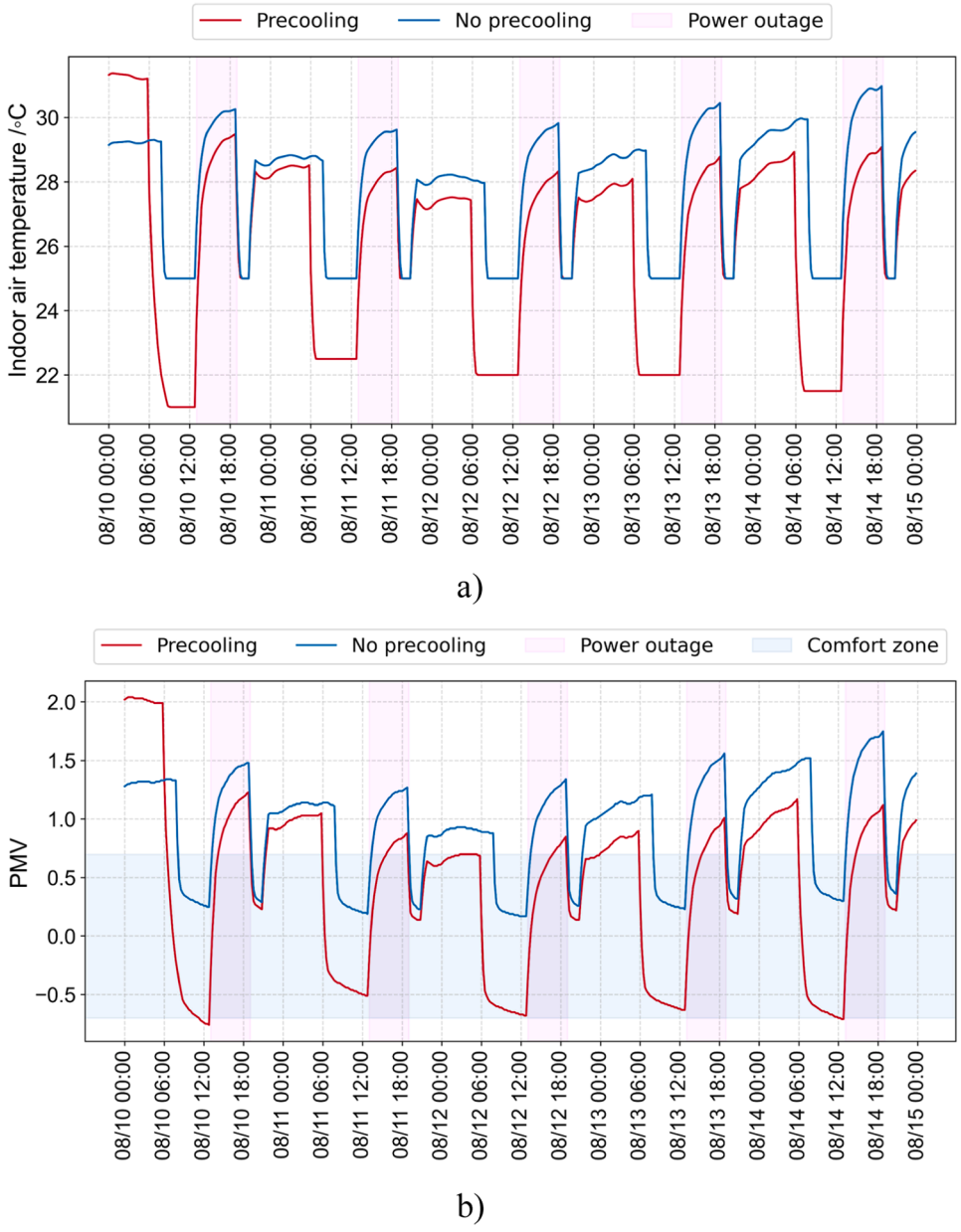

Fig. 10. a) Indoor air temperature and b) PMV profiles of precooling and without precooling during Event 2 (power outage: 13:00–19:00).

the sensitivity of the building design parameters varied little with cooling capacity. Airtightness remained the most influential factor, followed by the external wall insulation, whereas the effects of the other parameters were negligible.

4.3. Interactions between cooling capacity and internal thermal mass

This section further investigates the interaction between the cooling capacity and internal thermal mass during precooling. The selection of the internal thermal mass was categorized into three levels—low, medium, and high—corresponding to cases where the surface area of the internal thermal mass was set to one, two, and four times the floor area, respectively. For cooling capacity, five representative values were considered: 1.8, 2.7, 3.6, 4.5, and 5.4 kW. By combining these two parameters, 15 configurations were simulated to evaluate the thermal discomfort during the outage period under Event 3.

The results are illustrated by the heatmap in Fig. 14. The most severe thermal discomfort occurred under the combination of the lowest cooling capacity and lowest internal thermal mass, with a PMVCE of 13.38 h, while the combination of the highest cooling capacity and high internal thermal mass minimized thermal discomfort, reducing PMVCE to 0.38 h, highlighting the importance of coordinating cooling capacity with internal thermal mass. The figure shows that a higher internal thermal mass consistently reduced the PMVCE at a given cooling capacity. Similarly, for a fixed internal thermal mass, increasing the cooling capacity reduces the PMVCE. However, the marginal benefits diminish once the cooling capacity exceeds 4.5 kW, because further increases provide little additional reduction in thermal discomfort. For example, at a cooling capacity of 5.4 kW combined with a high internal thermal mass, the PMVCE reached 0.38, which is only slightly lower than that 0.40 observed at 4.5 kW, representing a 5 % reduction. This indicates that, beyond this point, increasing the cooling capacity yields minimal additional improvement in mitigating thermal discomfort.

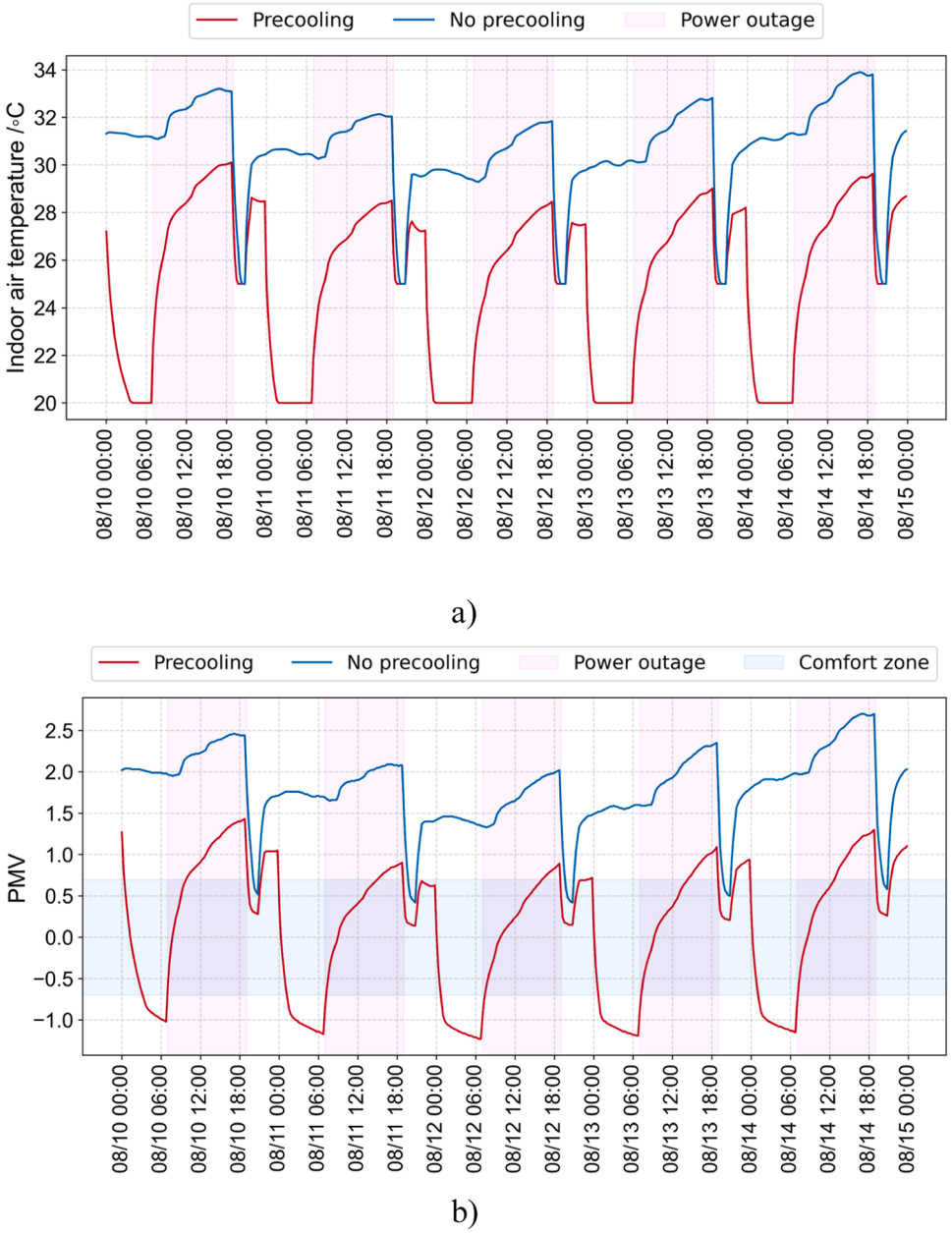

Fig. 11. a) Indoor air temperature and b) PMV profiles of precooling and without precooling during Event 3 (power outage: 7:00–19:00).

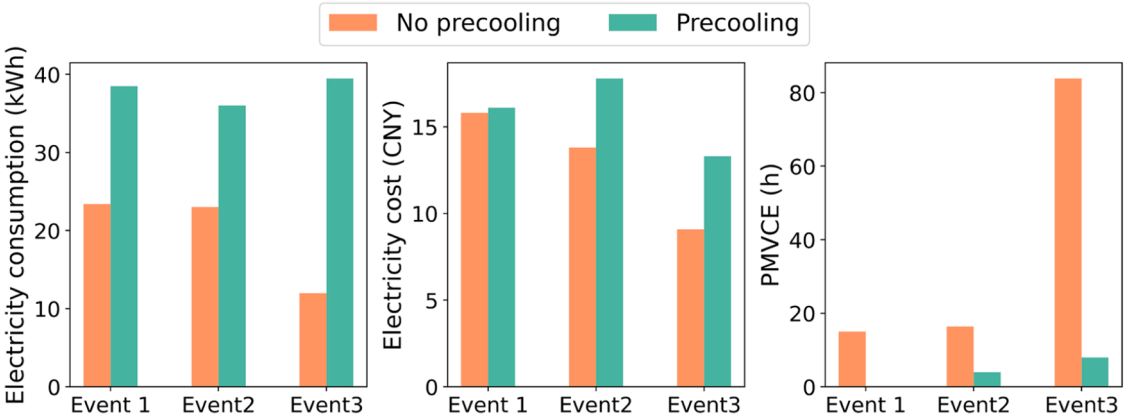

Fig. 12. Electricity consumption, electricity cost, and thermal discomfort during the two power-outage events.

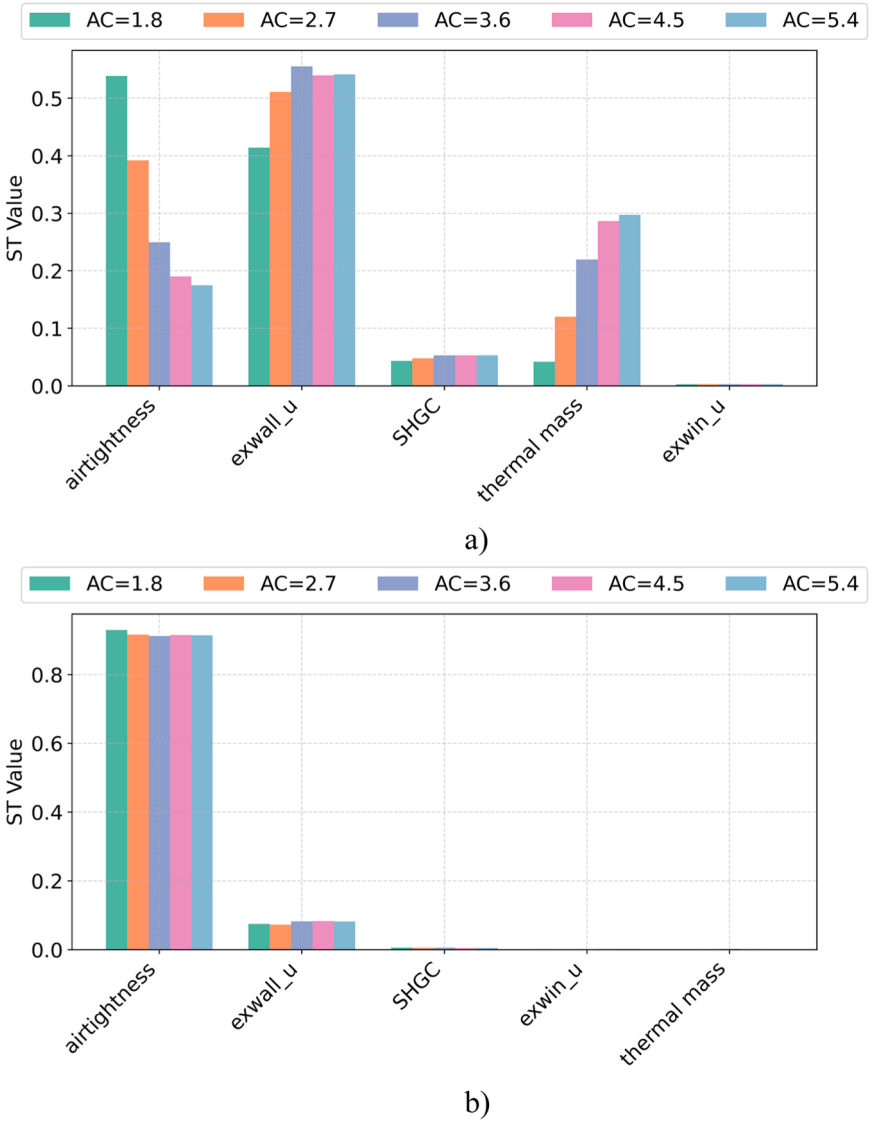

Fig. 13. Sensitivity variation of the input parameters for a) **thermal discomfort during power outage** and b) electricity cost (**CNY**).

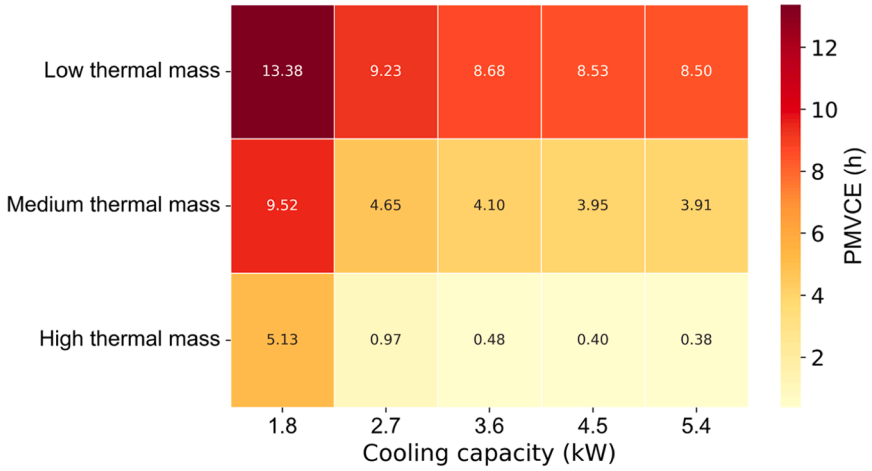

Fig. 14. PMVCE heat map under various cooling capacities and internal thermal mass levels.

4.4. Implications for enhancing precooling effectiveness

The sensitivity analysis and simulation results provide valuable insights for the effective implementation of precooling strategies in residential buildings. These implications can be summarized at three complementary levels: building envelope retrofitting, occupant behavior, and demand-side management during power outages.

4.4.1. Building envelope improvements

Sensitivity analysis indicated that external wall insulation has a dominant impact on the effectiveness of precooling strategies, particularly in mitigating thermal discomfort during power outages. The external walls of several existing residential buildings suffer from poor thermal performance owing to aging, material degradation, and the absence of insulation [43,44]. This low thermal resistance leads to a rapid indoor temperature rise and increased cooling energy losses, undermining both the energy efficiency and practical benefits of precooling. Therefore, enhancing the external wall insulation in aging residential communities is crucial. This can reduce heating and cooling energy consumption while improving the resilience and effectiveness of precooling strategies during heatwave events. In the context of urban renewal, promoting insulation retrofits of external walls provides a dual benefit by supporting sustainable energy upgrades and enabling the successful implementation of advanced cooling measures, such as precooling.

4.4.2. Occupant behavior advice

The sensitivity analysis also highlighted that building airtightness plays a critical role in reducing cooling electricity consumption. Poor airtightness can lead to uncontrolled infiltration through open windows, door gaps, and shared ventilation shafts. Improving airtightness reduces cooling demand and financial burden and prolongs the duration of thermal comfort during subsequent outages. Residents can take practical measures, such as keeping windows and doors closed, minimizing the airflow between rooms with different thermal conditions, and avoiding frequent door or window operations. By limiting this airflow, the precooling effect can be better preserved, thereby improving indoor thermal comfort and reducing overheating risks during critical periods.

4.4.3. Demand-side management of power outages

Even with precooling, the timing and duration of power outages critically affect indoor thermal conditions. Simulation results under the precooling scenario show that if outages occur in the morning (starting at 07:00), residents can tolerate up to 6 h without severe thermal discomfort, whereas afternoon outages (starting at 13:00) should not exceed 2 h. This difference can be primarily explained by solar heat gain dynamics. As shown in Fig. C1, during afternoon power-outage event, solar heat gains transmitted through exterior windows reach a peak around 13:00–14:00 and subsequently remain at a relatively high level, leading to the cooling energy stored earlier in the morning to be rapidly depleted once the power outage occurs in the afternoon. This is also reflected in the indoor temperature response: within the first hour after the outage, indoor temperature rises by approximately 6.6 °C for the afternoon event, whereas the corresponding rise is only about 4.3 °C for the morning event. In addition, precooling performed in the morning inherently competes against rising outdoor temperatures and increasing solar heat gains, meaning that part of the cooling energy is consumed rather than stored within the thermal mass. As a result, a morning outage generally benefits more from precooling compared with an afternoon outage.

Therefore, if a power outage is unavoidable, demand-side management strategies should account for the outage timing and provide residents with advance notice, enabling them to precool their homes [28,45,46]. Careful scheduling of outages and informing households in advance can significantly reduce overheating risks during heatwaves.

4.5. Limitations and future work

This study has several limitations. Fixed occupancy schedules and typical internal heat gains were adopted to simulate the indoor air temperature and cooling electricity consumption, which may not fully capture the stochastic nature of occupant behavior throughout the day. Future work should adopt stochastic occupancy models to better reflect actual occupant behavior. Second, the findings were based on a single high-rise residential case study located in Chengdu, which limits the generalizability of the results to other building types and climate zones. Comparative studies involving different building types and climate regions would help investigate and extend the applicability of the proposed precooling strategies. In addition, this study assumed that natural ventilation remained closed in the target room, primarily based on the consideration that occupants are likely to keep windows shut to maintain indoor comfort during power outages. However, window-opening behavior can be uncertain in residential buildings, and natural ventilation may influence the effectiveness of precooling [47]. Therefore, future work is needed to quantitatively evaluate precooling performance under stochastic window-opening behaviors and natural ventilation scenarios. Finally, the performances of the precooling strategies were evaluated through numerical simulations. A direct comparison with existing studies was not conducted because most prior work focuses on normal power-supply conditions, in which AC systems remain continuously operated, and the building is not in a free-floating mode. Therefore, the research scenario and boundary conditions in this study differ from those in existing literature. Future studies should include field experiments to verify the accuracy of the simulated results and assess the practical effectiveness of the optimized precooling strategies in residential buildings.

5. Conclusions

This study investigated the effectiveness of adopting an optimized precooling strategy in a prototype residential building during heatwaves with power outages. A Bayesian optimization algorithm was employed to develop a precooling thermostat setpoint schedule aimed at minimizing both indoor overheating and cooling energy costs. Subsequently, the impacts of the building design parameters were evaluated using global sensitivity analysis, and the effects of cooling capacity and power-outage event characteristics were explored through parametric analysis. Over 3000 scenarios were simulated using the Sobol method. The significant findings are summarized as follows.

1) The optimized precooling strategy demonstrated the most effective mitigation of thermal discomfort compared with both the baseline and fixed cooling schedules. In particular, indoor air temperature was maintained below 27 °C during the outage, with peak temperature reductions of up to 3.5 °C compared to the baseline and 1.7 °C compared to the fixed strategy. However, the total electricity costs did not increase significantly.
2) Sensitivity analysis revealed the distinct primary factors influencing thermal discomfort and electricity costs. Thermal discomfort was dominated by the external wall insulation, airtightness and internal thermal mass. Notably, external wall insulation consistently played a critical role in thermal discomfort mitigation across different cooling capacity levels. In contrast, the electricity cost was primarily governed by airtightness, whereas the influence of other parameters was relatively small. This result highlights the significance of maintaining good room airtightness during power outages in reducing thermal discomfort and electricity costs, and provides practical guidance for occupant behavior.
3) An interaction between cooling capacity and internal thermal mass was observed. Specifically, as the capacity increased, the effect of the internal thermal mass became more significant while that of airtightness diminished. The combination of the lowest cooling

capacity and lowest internal thermal mass resulted in the most severe thermal discomfort, with a PMVCE of 13.38 h, whereas the combination of the highest cooling capacity and internal thermal mass produced the lowest thermal discomfort, with a PMVCE of 0.38 h. However, when capacity exceeded a certain threshold (4.5 kW in this study), further increases provided only marginal benefits, suggesting that coordinated optimization of both parameters is more effective than simply oversizing the cooling system.

4) The precooling performance was influenced by the timing and duration of power- outage events. Specifically, morning outages can last up to approximately 6 h without causing severe thermal discomfort, whereas afternoon outages should be limited to no more than 2 h. In terms of electricity costs, for a morning outage lasting 6 h, implementing precooling did not result in a significant increase compared with no precooling. However, for afternoon outages, the electricity costs increased by 28 %, and for morning outages extending up to 12 h, the costs increased by 46 %.

This study demonstrates the potential of applying precooling strategies to residential buildings during heatwaves with power outage events. The findings provide methodological support and behavioral guidance for mitigating overheating risks using precooling under heatwave conditions and power outages.

CRediT authorship contribution statement

Xue Liu: Writing – review & editing, Writing – original draft, Visualization, Software, Methodology, Funding acquisition, Conceptualization. **Hao Tang:** Writing – review & editing, Software, Methodology. **Xuyuan Kang:** Writing – review & editing, Software, Methodology. **Pengyuan Shen:** Writing – review & editing, Supervision. **Xin Zhou:** Writing – review & editing, Validation. **Da Yan:** Writing – review & editing, Supervision, Funding acquisition.

Declaration of competing interest

The authors declare that they have no known competing financial interests or personal relationships that could have appeared to influence the work reported in this paper.

Acknowledgements

This research was supported by the National Natural Science Foundation of China (Grant Numbers 52225801, 52408132, and 52308100) and the Fundamental Research Funds for the Central Universities (Grant Numbers 2682024CX072 and 2682024CX071).

Appendix A. Impact of internal heat gain on precooling performance

To analyze the effect of internal heat gains on precooling performance, the internal heat gains from occupants, lighting, and equipment were increased by 10 % relative to the default settings. The optimized precooling schedule during the selected heatwave period is in Table A1. Compared with the precooling schedule obtained under the original settings, small changes in precooling schedules were observed on August 11, 12, and 13, namely a 0.5-hour increase in the precooling duration and a 0.5 °C decrease of the setpoint. This means that increasing internal heat gains by 10 % leads to a slightly higher precooling intensity. For thermal comfort during power outage, indoor temperature profiles remain largely unchanged, as shown in Fig. A1, indicating that the tolerance duration during power outages is only minimally affected. This outcome can be explained by the fact that internal gains primarily come from occupants, whereas lighting and plug-load equipment cease operation during power outages and therefore do not contribute additional heat.

Table A1
The schedule of the optimized precooling strategy.

Date	Temperature setpoint (°C)	Precooling time (h)
2022/8/10	20	7
2022/8/11	20.5	5.5
2022/8/12	20.5	4
2022/8/13	20.5	7
2022/8/14	20	7

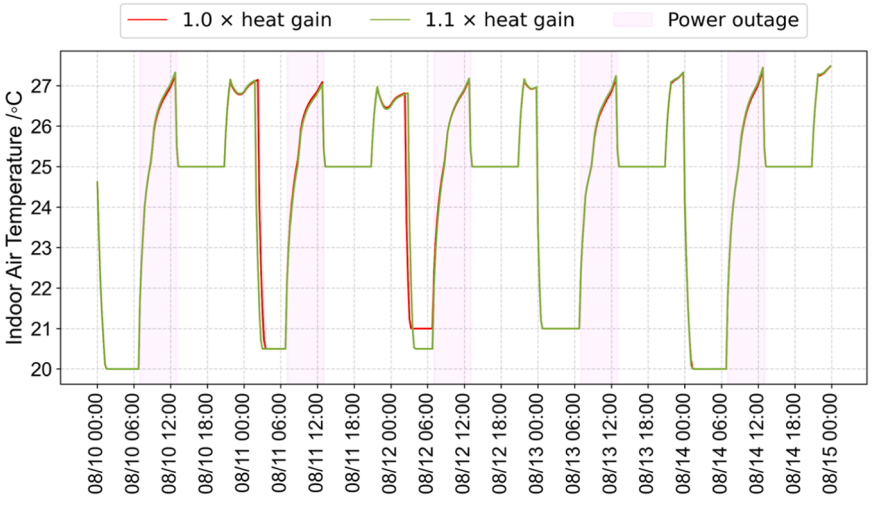

Fig. A1. Indoor air temperature profiles under two internal heat gain scenarios.

Appendix B. Influence of objective function weights

To evaluate how the weighting between thermal discomfort during power outages and electricity cost influences the precooling performance, a sensitivity analysis was conducted by varying the weighting coefficients of the two objectives. The weighting coefficients w_1 and w_2 correspond to thermal discomfort and electricity cost. Across scenarios 1 to 4, the value of w_1 increases from 0.5 to 0.8, while w_2 decreases from 0.5 to 0.2 accordingly. This shift reflects the fact that, during outage periods, maintaining habitable indoor conditions is essential for occupants' thermal safety, while electricity cost becomes a secondary concern. For each configuration, the corresponding optimized precooling strategy was obtained, and the results are presented in Table B1.

These results reveal that even under the default setting with equal weight configuration ($w_1 = w_2 = 0.5$), thermal discomfort was already reduced to a relatively low level, with *PMVCE* of 0.76 h. When the comfort weighting increased, *PMVCE* decreased to 0.52 h, indicating a moderate improvement. However, further increasing the comfort weighting did not lead to additional reductions. Regarding electricity cost, it remained nearly unchanged across all weighting configurations. This finding indicates that thermal discomfort and electricity cost may not be in a strict trade-off relationship. Instead, there exists a zone of synergy where precooling simultaneously improve thermal comfort without incurring additional energy cost. As a result, adjusting the weighting coefficients does not dramatically change the optimal solution.

Table B1
Precooling performance of four weighting configurations.

Configuration	w_1	w_2	Electricity cost (CNY)	*PMVCE* (h)
1	0.5	0.5	16.28	0.76
2	0.6	0.4	16.27	0.58
3	0.7	0.3	16.26	0.52
4	0.8	0.2	16.27	0.52

Appendix C. Heat gain dynamics of window solar radiation and wall convection

To further explain the differences in precooling performance observed between the two power-outage events, heat-flux related outputs were exported from the simulation. Specifically, heat gain rates per unit area of window-transmitted solar radiation and interior wall-surface convection were extracted and analyzed to clarify their combined influence on precooling performance, as shown in Fig. C1. The window-transmitted solar radiation rate begins increasing shortly after sunrise and reaches a peak of approximately 12 W/m^2 around 13:00–14:00, while remaining at a relatively high level for several hours in the afternoon. However, the wall-surface convection heat gain rate is much smaller in magnitude and rises more slowly during the power outage period. It should be noted that positive values of the wall convection heat gain rate indicate that heat transferred from the wall into the indoor air, whereas negative values reflect heat being absorbed by the wall.

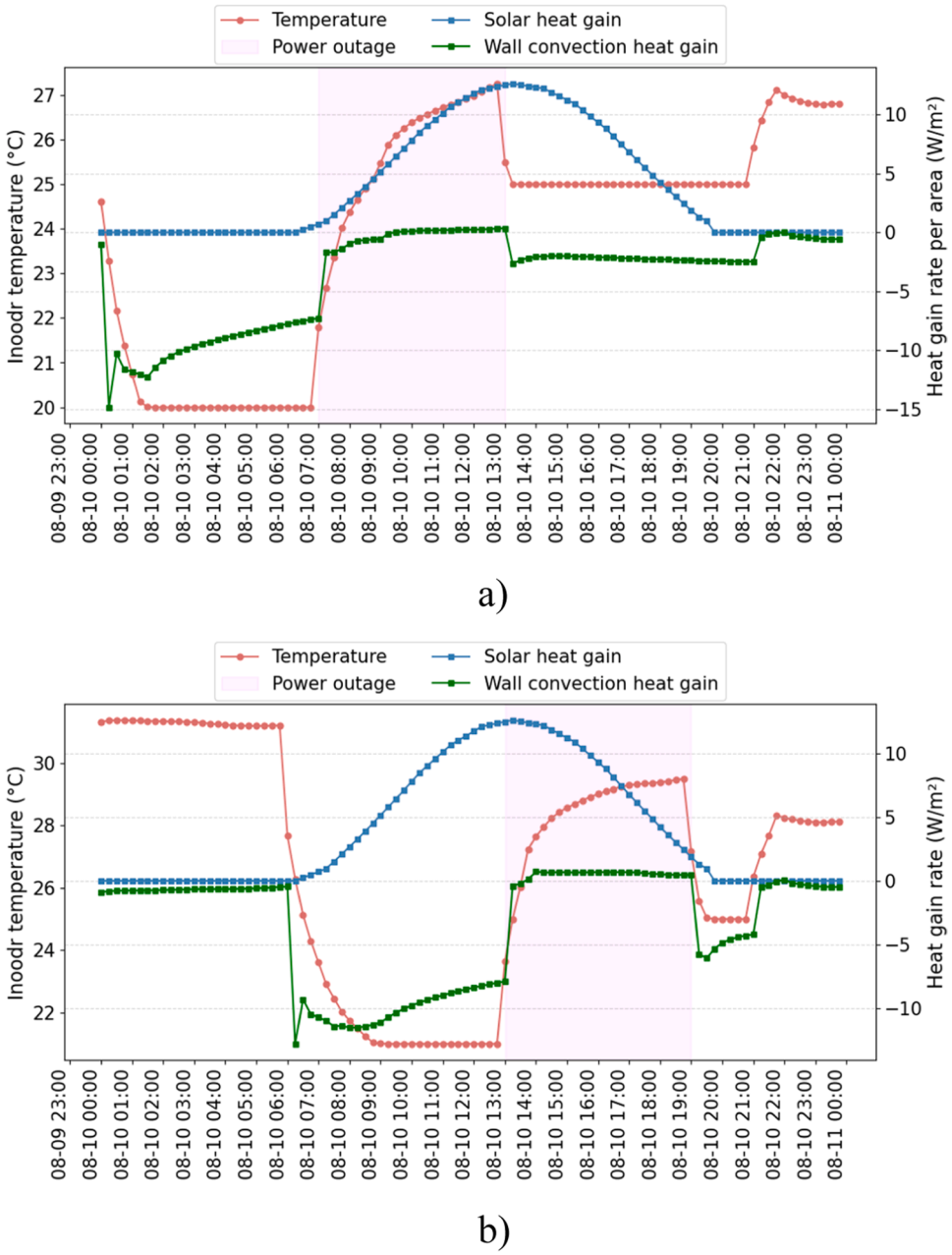

Fig. C1. Heat gain rates of window-transmitted solar radiation and exterior wall convection under a) Event 1 and b) Event 2.

Data availability

Data will be made available on request.

References

[1] National Oceanic and Atmospheric Administration, Climate change: global temperature, 2025. https://www.climate.gov/news-features/understanding-climate/climate-change-global-temperature. accessed August 8, 2025.

[2] J. Ballester, M. Quijal-Zamorano, R.F. Méndez Turrubiates, F. Pegenaute, F. R. Herrmann, J.M. Robine, X. Basagaña, C. Tonne, J.M. Antó, H. Achebak, Heat-related mortality in Europe during the summer of 2022, Nat. Med. 29 (2023) 1857–1866, https://doi.org/10.1038/s41591-023-02419-z.

[3] China Meteorological Administration, China Climate Bulletin (2022), Beijing, 2022. https://www.cma.gov.cn/zfxxgk/gknr/qxbg/202303/t20230324_5396394.html.

[4] J. Liang, Y. (Lucy) Qiu, B. Wang, X. Shen, S. Liu, Impacts of heatwaves on electricity reliability: evidence from power outage data in China, IScience 28 (2025) 111855, https://doi.org/10.1016/j.isci.2025.111855.

[5] S. Zhang, C. Zhang, W. Cai, Y. Bai, M. Callaghan, N. Chang, B. Chen, H. Chen, L. Cheng, H. Dai, X. Dai, W. Fan, X. Fang, T. Gao, Y. Geng, D. Guan, Y. Hu, J. Hua, C. Huang, H. Huang, J. Huang, X. Huang, J.S. Ji, Q. Jiang, X. Jiang, G. Kiesewetter, T. Li, L. Liang, B. Lin, H. Lin, H. Liu, Q. Liu, X. Liu, Z. Liu, Z. Liu, Y. Liu, B. Lu, C. Lu, Z. Luo, W. Ma, Z. Mi, C. Ren, M. Romanello, J. Shen, J. Su, Y. Sun, X. Sun, X. Tang, M. Walawender, C. Wang, Q. Wang, R. Wang, L. Warnecke, W. Wei, S. Wen, Y. Xie, H. Xiong, B. Xu, Y. Yan, X. Yang, F. Yao, L. Yu, J. Yuan, Y. Zeng, J. Zhang, L. Zhang, R. Zhang, S. Zhang, S. Zhang, M. Zhao, D. Zheng, H. Zhou, J. Zhou, Z. Zhou, Y. Luo, P. Gong, The 2023 China report of the Lancet Countdown on health and climate change: taking stock for a thriving future, Lancet Public Heal. 8 (2023) e978–e995, https://doi.org/10.1016/S2468-2667(23)00245-1.

[6] X. Basagaña, C. Sartini, J. Barrera-Gómez, P. Dadvand, J. Cunillera, B. Ostro, J. Sunyer, M. Medina-Ramón, Heat waves and cause-specific mortality at all ages, Epidemiology 22 (2011). https://journals.lww.com/epidem/fulltext/2011/11000/heat_waves_and_cause_specific_mortality_at_all.2.aspx.

[7] J. Cheng, Z. Xu, H. Bambrick, H. Su, S. Tong, W. Hu, Heatwave and elderly mortality: an evaluation of death burden and health costs considering short-term mortality displacement, Env. Int. 115 (2018) 334–342, https://doi.org/10.1016/j.envint.2018.03.041.
[8] K. Sun, M. Specian, T. Hong, Nexus of thermal resilience and energy efficiency in buildings: a case study of a nursing home, Build. Env. 177 (2020) 106842, https://doi.org/10.1016/j.buildenv.2020.106842.
[9] M. Sheng, M. Reiner, K. Sun, T. Hong, Assessing thermal resilience of an assisted living facility during heat waves and cold snaps with power outages, Build. Env. 230 (2023) 110001, https://doi.org/10.1016/j.buildenv.2023.110001.
[10] X. Liu, Z. Liu, Y. Wu, S. Hu, F. Bu, J. An, X. Zhou, D. Yan, A novel quantitative method of heatwave classification for building resilience analysis, Sustain, Cities Soc. 112 (2024) 105603, https://doi.org/10.1016/j.scs.2024.105603.
[11] S. Attia, R. Levinson, E. Ndongo, P. Holzer, O. Berk Kazanci, S. Homaei, C. Zhang, B.W. Olesen, D. Qi, M. Hamdy, P. Heiselberg, Resilient cooling of buildings to protect against heat waves and power outages: key concepts and definition, Energy Build. 239 (2021) 110869, https://doi.org/10.1016/j.enbuild.2021.110869.
[12] R. Yin, E.C. Kara, Y. Li, N. DeForest, K. Wang, T. Yong, M. Stadler, Quantifying flexibility of commercial and residential loads for demand response using setpoint changes, Appl. Energy 177 (2016) 149–164, https://doi.org/10.1016/j.apenergy.2016.05.090.
[13] S. Naderi, G. Pignatta, S. Heslop, I. Macgill, D. Chen, Demand response via pre-cooling and solar pre-cooling : a review, Energy Build. 272 (2022) 112340, https://doi.org/10.1016/j.enbuild.2022.112340.
[14] W.J.N. Turner, I.S. Walker, J. Roux, Peak load reductions: electric load shifting with mechanical pre-cooling of residential buildings with low thermal mass, Energy 82 (2015) 1057–1067, https://doi.org/10.1016/j.energy.2015.02.011.
[15] H. Stopps, M.F. Touchie, Load shifting and energy conservation using smart thermostats in contemporary high-rise residential buildings: estimation of runtime changes using field data, Energy Build. 255 (2022) 111644, https://doi.org/10.1016/j.enbuild.2021.111644.
[16] H. Stopps, M.F. Touchie, Perceptions of thermal conditions in contemporary high-rise apartment buildings under different temperature control strategies, Sci. Technol. Built. Env. 27 (2021) 1492–1504, https://doi.org/10.1080/23744731.2021.1929465.
[17] J. Wang, C. Yik, L. Song, Analysis of precooling optimization for residential buildings, Appl. Energy 323 (2022) 119574, https://doi.org/10.1016/j.apenergy.2022.119574.
[18] Y. Jiang, K. Andrew, J. Wang, C. Yik, L. Song, Development, implementation, and impact analysis of model predictive control-based optimal precooling using smart home thermostats, Energy Build. 303 (2024) 113790, https://doi.org/10.1016/j.enbuild.2023.113790.
[19] J. Wang, Z. Wei, Y. Zhu, C. Zheng, B. Li, X. Zhai, Demand response via optimal pre-cooling combined with temperature reset strategy for air conditioning system: a case study of office building, Energy 282 (2023) 128751, https://doi.org/10.1016/j.energy.2023.128751.
[20] X. Lu, V.A. Adetola, S. Bhattacharya, Large-scale simulation-based parametric analysis of an optimal precooling strategy for demand flexibility in a commercial office building, Energy Build. 316 (2024) 114284, https://doi.org/10.1016/j.enbuild.2024.114284.
[21] X. Liu, X. Liu, Y. Geng, D. Yan, S. Hu, H. Tang, A Bayesian–physics integrated optimization framework for flexible building cooling under heatwave conditions, Energy Build. 348 (2025) 116466, https://doi.org/10.1016/j.enbuild.2025.116466.
[22] A. Xu, C. Song, W. Zhao, Y. Chen, Demand flexibility of pre-cooling strategies for city-scale buildings through urban building energy modeling, Buildings 15 (2025), https://doi.org/10.3390/buildings15071051.
[23] J. Wang, C. Yik, L. Song, Design and analysis of optimal pre-cooling in residential buildings, Energy Build. 216 (2020) 109951, https://doi.org/10.1016/j.enbuild.2020.109951.
[24] R. Yin, P. Xu, M.A. Piette, S. Kiliccote, Study on auto-DR and pre-cooling of commercial buildings with thermal mass in California, Energy Build. 42 (2010) 967–975, https://doi.org/10.1016/j.enbuild.2010.01.008.
[25] Y. Chen, P. Xu, Z. Chen, H. Wang, H. Sha, Y. Ji, Y. Zhang, Q. Dou, S. Wang, Experimental investigation of demand response potential of buildings: combined passive thermal mass and active storage, Appl. Energy 280 (2020) 115956, https://doi.org/10.1016/j.apenergy.2020.115956.
[26] R. Arababadi, M. Elzomor, K. Parrish, Selection of energy efficiency measures to enhance the effectiveness of pre-cooling in residential buildings in hot arid climate Selection of energy efficiency measures to enhance the effectiveness of pre-cooling in residential buildings in hot arid clima, Sci. Technol. Built Env. 0 (2016) 1–10, https://doi.org/10.1080/23744731.2016.1262660.
[27] Z. Zeng, W. Zhang, K. Sun, M. Wei, T. Hong, Investigation of pre-cooling as a recommended measure to improve residential buildings' thermal resilience during heat waves, Build. Env. 210 (2022) 108694, https://doi.org/10.1016/j.buildenv.2021.108694.
[28] Z. Wang, T. Hong, H. Li, Informing the planning of rotating power outages in heat waves through data analytics of connected smart thermostats for residential buildings, Env. Res. Lett. 16 (2021), https://doi.org/10.1088/1748-9326/ac092f.
[29] China Meteorological Administration, The definition of heat waves, 2011 h.t.tps://w.w.w.cma.gov.cn/2011qxfw/2011qqxkp/2011qkpdt/201110/t20111026_124192.htmlaccessed August 8, 2025.
[30] H. Hersbach, B. Bell, P. Berrisford, A. Horányi, J.M. Sabater, J. Nicolas, R. Radu, D. Schepers, A. Simmons, C. Soci, D. Dee, Global reanalysis: goodbye ERA-interim, hello ERA5, ECMWF Newsl. (2019) 17–24.
[31] J. An, Y. Wu, C. Gui, D. Yan, Chinese prototype building models for simulating the energy performance of the nationwide building stock, Build. Simul. (2023) 1559–1582, https://doi.org/10.1007/s12273-023-1058-5.
[32] X. Liu, S. Hu, D. Yan, A statistical quantitative analysis of the correlations between socio-demographic characteristics and household occupancy patterns in residential buildings in China, Energy Build. 284 (2023) 112842, https://doi.org/10.1016/j.enbuild.2023.112842.
[33] Z. Chen, J. Wen, S.T. Bushby, L.J. Lo, Z.O. Neill, W.V. Payne, A. Pertzborn, C. Calfa, Y. Fu, G. Grajewski, Y. Li, Z. Yang, An analysis of the hybrid internal mass modeling approach in EnergyPlus, 12th ESim build. Simul. Conf. Ott. Can. (2022).
[34] International Organization for Standardization, ISO 7730: ergonomics of the thermal environment — analytical determination and interpretation of thermal comfort using calculation of the PMV and PPD indices and local thermal comfort criteria, ISO, 2005.
[35] M. Pelikan, in: M. Pelikan (Ed.), Bayesian optimization algorithm BT - hierarchical bayesian optimization algorithm: toward a new generation of evolutionary algorithms, Springer Berlin Heidelberg, Berlin, Heidelberg, 2005, pp. 31–48, https://doi.org/10.1007/978-3-540-32373-0_3.
[36] P. Heiselberg, H. Brohus, A. Hesselholt, H. Rasmussen, E. Seinre, S. Thomas, Application of sensitivity analysis in design of sustainable buildings, Renew. Energy 34 (2009) 2030–2036, https://doi.org/10.1016/j.renene.2009.02.016.
[37] I.M. Sobol′, Global sensitivity indices for nonlinear mathematical models and their Monte Carlo estimates, Math. Comput. Simul. 55 (2001) 271–280, https://doi.org/10.1016/S0378-4754(00)00270-6.
[38] A. Saltelli, M. Ratto, F.Terry Andres, Glob. Sensit. Anal. Primer (2007), https://doi.org/10.1002/9780470725184.ch4.
[39] J. Hou, Y. Sun, Q. Chen, R. Cheng, J. Liu, X. Shen, H. Tan, H. Yin, K. Huang, Y. Gao, X. Dai, L. Zhang, B. Liu, J. Sundell, Air change rates in urban Chinese bedrooms, Indoor Air. 29 (2019) 828–839, https://doi.org/10.1111/ina.12582.
[40] T. HOMMA, A. SALTELLI, Use of Sobol's quasirandom sequence generator for integration of modified uncertainty importance measure, J. Nucl. Sci. Technol. 32 (1995) 1164–1173, https://doi.org/10.1080/18811248.1995.9731832.
[41] J. Herman, W. Usher, SALib : sensitivity analysis library in Python (Numpy). Contains sobol, SALib : an open-source Python library for sensitivity analysis, J. Open Source Softw. 2 (2017) 97, https://doi.org/10.1016/S0010-1.
[42] S. Naderi, S. Heslop, D. Chen, I. Macgill, G. Pignatta, Consumer cost savings, improved thermal comfort, and reduced peak air conditioning demand through pre-cooling in Australian housing, Energy Build. 271 (2022) 112172, https://doi.org/10.1016/j.enbuild.2022.112172.
[43] K. Sun, W. Zhang, Z. Zeng, R. Levinson, M. Wei, T. Hong, Passive cooling designs to improve heat resilience of homes in underserved and vulnerable communities, Energy Build. 252 (2021) 111383, https://doi.org/10.1016/j.enbuild.2021.111383.
[44] Z. Liu, X. Zhou, W. Tian, X. Liu, D. Yan, Impacts of uncertainty in building envelope thermal transmittance on heating/cooling demand in the urban context, energy Build. 273 (2022) 112363. 10.1016/j.enbuild.2022.112363.
[45] D. Lowe, K.L. Ebi, B. Forsberg, Heatwave early warning systems and adaptation advice to reduce human health consequences of heatwaves, Int. J. Env. Res. Public Health 8 (2011) 4623–4648, https://doi.org/10.3390/ijerph8124623.
[46] M.A. Palecki, S.A. Changnon, K.E. Kunkel, The nature and impacts of the July 1999 heat wave in the midwestern United States: learning from the lessons of 1995, Bull. Am. Meteorol. Soc. 82 (2001) 1353–1367, https://doi.org/10.1175/1520-0477(2001)082. <1353:TNAIOT>2.3.CO;2.
[47] S. Koley, Examining thermal properties of cross-ventilation in multizone buildings : machine learning appraisal of modelling methods and architectural ingenuities, Int. J. Eng. Trends Technol. 73 (2025) 364–416.